Chinese Chemical Letters 24 (2013) 145–148

Contents lists available at SciVerse ScienceDirect

Chinese Chemical Letters

journal homepage: www.elsevier.com/locate/cclet

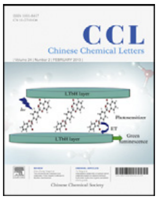

Original article

Excited-state charge coupled proton transfer reaction *via* the dipolar functionality of salicylideneaniline

Tzu-Chien Fang, Hsing-Yang Tsai, Ming-Hui Luo, Che-Wei Chang, Kew-Yu Chen *

Department of Chemical Engineering, Feng Chia University, Taichung 40724, Taiwan

A R T I C L E I N F O

Article history:
Received 27 September 2012
Received in revised form 5 December 2012
Accepted 14 December 2012
Available online 4 February 2013

Keywords:
ESIPT
ESICT
Dipolar functionality
Salicylideneaniline derivatives

A B S T R A C T

Based on design and synthesis of salicylideneaniline derivatives (**1a**–**1d**), we demonstrate a prototypical system to investigate the excited-state intramolecular charge transfer (ESICT) coupled excited-state intramolecular proton transfer (ESIPT) reaction *via* the dipolar functionality of the molecular framework. In solid and aprotic solvents **1a**–**1d** exist mainly as *E* conformers that possess an intramolecular six-membered-ring hydrogen bond. Compounds **1a**–**1c** exhibit a unique proton-transfer tautomer emission, while compound **1d** exhibits remarkable dual emission due to the different solvent-polarity environment between ESICT and ESIPT states. Time-dependent density functional theory (TDDFT) calculations are reported on these Schiff bases in order to rationalize their electronic structure and absorption spectra.

1. Introduction

Schiff bases are some of the most widely used organic compounds [1–6]. They are used as dyes and pigments [7–11], catalysts [12–14], liquid crystals [15–17], and intermediates in organic synthesis [18–22]. Moreover, several Schiff bases exhibit a broad range of biological activities [23]. For example, salicylideneaniline derivatives are effective against *Mycobacterium tuberculosis* H37Rv [24]. The excited-state intramolecular proton transfer (ESIPT) reaction of salicylideneaniline derivatives [25,26], which incorporates transfer of a hydroxy proton to the imine nitrogen through an intramolecular six-membered-ring hydrogen-bonding system, has been investigated in the past. The proton transfer dyes have found many important applications. Typical examples include probes for solvation dynamics [27] and biological environments [28], photochromic materials [29], chemosensors [30–32], and organic light-emitting diodes [33]. Furthermore, several relevant examples have recently been explored by anchoring the ESIPT molecules with a strong electron-donating substituent such as dialkylamines, so that upon Franck–Condon excitation, excited-state intramolecular charge transfer (ESICT) may take place. In an effort to probe this fundamental issue, studies of the ESIPT reaction in 2-hydroxy-4-(di-*p*-tolylamino)benzaldehyde and *N*,*N*-dialkyllamino-3-hydroxyflavone [34] have been carried out with femtosecond techniques to investigate the dynamics of the ESIPT reactions. Based on the chemical design, we herein demonstrate a practical approach to investigate the ESICT/ESIPT coupled reaction *via* the dipolar functionality of X-salicylidene-Y-aniline compounds with X = $N(CH_3)_2$ as an electron donor substituent and Y = CN as an electron acceptor substituent.

2. Experiment

*The general procedure for the synthesis of Schiff bases (***1a**–**1d***)*: Nonsubstituted/substituted aniline (5.4 mmol) and formic acid (0.1 mL) were added to a mixture of nonsubstituted/substituted 2-hydroxybenzaldehyde (4.7 mmol) and molecular sieves 4 Å (0.5 g) in ethanol (25 mL) at room temperature. The mixture was refluxed for 12 h. After cooling, the mixture was poured into the cold water and extracted with CH_2Cl_2 and dried with anhydrous $MgSO_4$. After solvent was removed, the crude product was purified by silica gel column chromatography with eluent CH_2Cl_2 to produce the title compounds (**1a**–**1d**) (Scheme 1) in 90% yield. Characterization data: **1a**: ^{1}H NMR (400 MHz, $CDCl_3$): δ 13.26 (br, 1H), 8.62 (s, 1H), 7.36–7.44 (m, 4H), 7.30–7.25 (m, 3H), 7.04 (d, 1H, *J* = 8.5 Hz), 6.96 (t, 1H, *J* = 7.5 Hz); MS (FAB) *m*/*z* (relative intensity) 198 (M+H$^+$, 100); HRMS calcd. for $C_{13}H_{12}NO$ 198.0919, found 198.0916. **1b**: ^{1}H NMR (400 MHz, $CDCl_3$): δ 12.60 (br, 1H), 8.59 (s, 1H), 7.71 (d, 2H, *J* = 8.0 Hz), 7.44 (m, 2H), 7.33 (d, 2H, *J* = 8.0 Hz), 7.03 (d, 1H, *J* = 8.5 Hz), 6.98 (t, 1H, *J* = 8.0 Hz); MS (FAB) *m*/*z* (relative intensity) 223 (M+H$^+$, 100); HRMS calcd. for $C_{14}H_{11}N_2O$ 223.0871, found 223.0875. **1c**: ^{1}H NMR (400 MHz, $CDCl_3$): δ 13.85 (br, 1H), 8.42

---

* Corresponding author.
E-mail address: kyuchen@fcu.edu.tw (K.-Y. Chen).

http://dx.doi.org/10.1016/j.cclet.2013.01.011

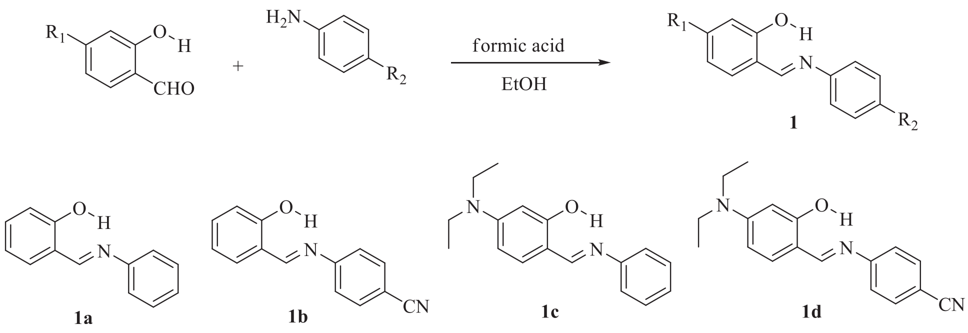

Scheme 1. The synthetic route of **1** and the structures of **1a**–**1d**.

(s, 1H), 7.15–7.40 (m, 6H), 6.26 (dd, 1H, J_1 = 8.5 Hz, J_2 = 2.0 Hz), 6.19 (s, 1H), 3.42 (q, 4H, J_1 = 7.0 Hz), 1.23 (t, 6H, J = 7.0 Hz); ^{13}C NMR (100 MHz, CDCl$_3$): δ 164.27, 160.41, 151.80, 148.77, 133.70, 129.21, 125.42, 120.73, 109.08, 103.72, 97.78, 44.55, 12.67; MS (FAB) *m*/*z* (relative intensity) 269 (M+H$^+$, 100); HRMS calcd. for $C_{17}H_{21}N_2O$ 269.1654, found 269.1650. Selected data for **1d**: ^{1}H-NMR (400 MHz, CDCl$_3$): δ 13.28 (br, 1H), 8.41 (s, 1H), 7.66 (d, 2H, J = 8.5 Hz), 7.28 (d, 2H, J = 8.5 Hz), 7.18 (d, 1H, J = 9.5 Hz), 6.29 (dd, 1H, J_1 = 9.5 Hz, J_2 = 2.5 Hz), 6.18 (d, 1H, J = 2.5 Hz), 3.44 (q, 4H, J = 7.5 Hz), 1.24 (t, 6H, J = 7.5 Hz); ^{13}C NMR (100 MHz, CDCl$_3$): δ 164.07, 162.13, 153.06, 152.54, 134.40, 133.38, 121.62, 119.12, 108.89, 108.21, 104.31, 97.52, 44.67, 12.65; MS (FAB) *m*/*z* (relative intensity) 294 (M+H$^+$, 100); HRMS calcd. for $C_{18}H_{20}N_3O$ 294.1606, found 294.1603.

3. Results and discussion

Scheme 1 shows the synthetic route of **1** and the structures of compounds **1a**–**1d**. These Schiff bases were prepared through condensation reactions between substituted salicylic aldehydes and substituted anilines [35]. The dominance of a *E* isomer for **1a**–**1d**, namely intramolecular hydrogen-bond formation between O–H and N, is firmly confirmed by single-crystal X-ray analyses [36–39]. In good agreement with these observations, the ^{1}H NMR spectra (in CDCl$_3$) revealed significantly downfield signals at $\delta > 12$ for all compounds **1a**–**1d**, giving a clear indication of the strong hydrogen-bond formation.

Fig. 1 shows the absorption and emission spectra of **1a**–**1c** in cyclohexane. Compound **1a** exhibits a $S_0 \rightarrow S_1$ electronic transition at 340 nm. The longest wavelength absorption band of **1b** (**1c**) is slightly red-shifted relative to that of **1a**; this can be explained by the fact that the addition of an electron-withdrawing group (electron-donating group) at the benzene (phenol) ring decreases (increases) the LUMO (HOMO) energy level and hence decreases the energy gap. As for the steady-state emission, **1a**–**1c** all exhibit solely a long wavelength emission (>540 nm) in cyclohexane. Fig. 1 clearly shows a large separation of the energy gap between the 0–0 onset of the absorption and emission. The Stokes shift of the emission, defined by peak (absorption)-to-peak (emission) gap in terms of frequency, is calculated to be >8500 cm^{-1} for **1a**–**1c**. Accordingly, the assignment of 540–575 nm emission for **1a**–**1c** in cyclohexane to a proton-transfer tautomer emission is unambiguous, and ESIPT takes place from the phenolic proton O–H to the imine nitrogen, forming the keto-amine tautomeric species.

Fig. 2 shows the absorption and emission spectra of **1d** in various solvents. It is apparent that the absorption spectrum of **1d** is a close resemblance to that of **1c**. Despite the similarity in absorption spectra, in which the $S_0 \rightarrow S_1$ peak wavelengths are both located at 370–390 nm for **1c** and **1d**, the corresponding emission reveals remarkable differences. In contrast to a unique proton-transfer emission in **1c**, dual emission maximized at 445 and 573 nm was observed for **1d** in cyclohexane. The 573 nm band can clearly be assigned to the keto-amine emission resulting from ESIPT, while the 445 nm band is absent in **1c** and is accordingly ascribed to the fluorescence of the enol-imine species.

As shown in Fig. 2, similar dual emission was observed for **1d** in other solvents. However, as the solvent polarity increases, the intensity ratio for the keto-amine *versus* enol-imine intensity decreases, approaching zero in acetonitrile. While the peak wavelength of the keto-amine emission remains unchanged, the enol-imine emission of **1d** reveals appreciable solvent-polarity dependence, being shifted from 445 nm in cyclohexane to 489 nm in acetonitrile. The fluorescence spectra shift significantly to the red upon increasing solvent polarity, indicating an intramolecular charge transfer characteristic for the excited state of **1d**. In view of the high electron affinity of the cyano group and the low ionization potential of the diethylamino group, the occurrence of ESICT in **1d** is expected.

To gain more insight into the electronic properties of **1a**–**1d**, quantum mechanical calculations were performed using

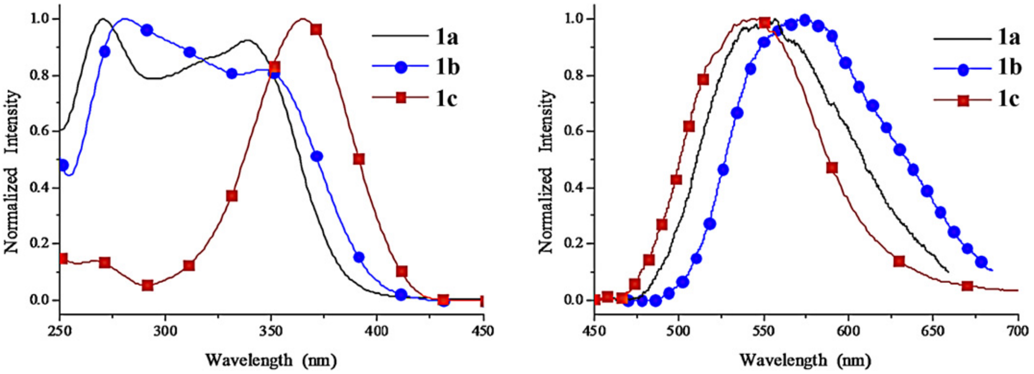

Fig. 1. Normalized absorption (left) and emission (right) spectra of **1a**, **1b** and **1c** in cyclohexane.

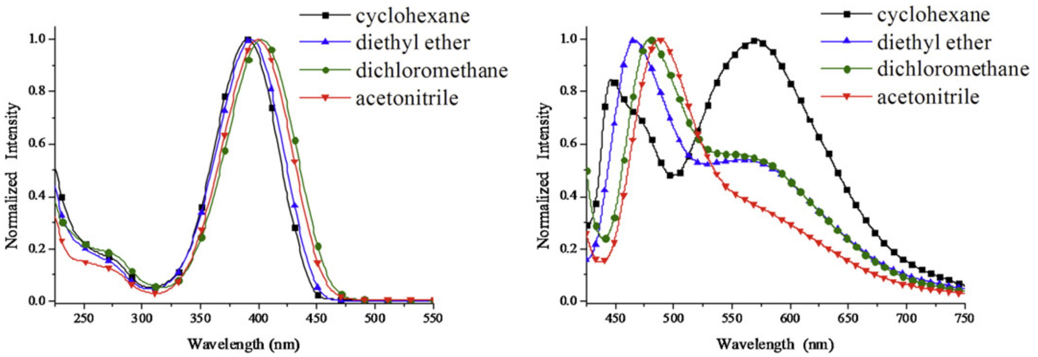

Fig. 2. Normalized absorption (left) and emission (right) spectra of **1d** in cyclohexane, diethyl ether, dichloromethane and acetonitrile.

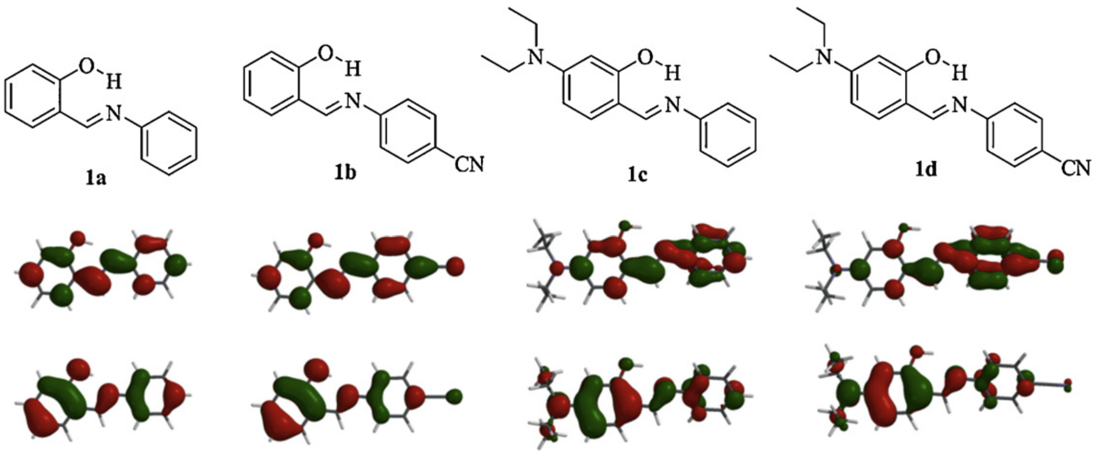

Fig. 3. Computed frontier orbitals of **1a**–**1d**. The upper graphs are the LUMOs and the lower ones are the HOMOs.

Table 1
Calculated (TDDFT/B3LYP) and experimental parameters for **1a–1d**.

Compound	HOMO[a]	LUMO[a]	Band gap[a]	f[a]	E_g [b]
1a	−6.02	−2.39	3.63	0.3537	3.66
1b	−6.11	−2.63	3.48	0.3548	3.57
1c	−5.25	−1.81	3.44	1.0334	3.40
1d	−5.29	−1.99	3.30	1.1569	3.18

f is the oscillator strength for the lowest energy transition.

[a] TDDFT/B3LYP calculated values.

[b] At absorption maxima ($E_g = 1240/\lambda_{max}$, in eV).

time-dependent density functional theory (TDDFT) at the B3LYP/6-31G** level. Fig. 3 shows the highest occupied molecular orbital (HOMO) and the lowest unoccupied molecular orbital (LUMO) of **1a**–**1d**. The HOMO (LUMO) in **1a**–**1c** is delocalized extensively over the whole π-conjugated system. However, the HOMO of **1d** is delocalized mainly on the amino group and the phenol ring, while the LUMO is extended from the imine group to the cyano substituent. The result reaffirms the viewpoint of ICT in **1d** from diethylamine to the cyano nitrogen. The calculated and experimental parameters for **1a**–**1d** are summarized in Table 1. The trend of the HOMO–LUMO energy gap is **1a** > **1b** > **1c** > **1d**, which is in good agreement with the theoretical calculations.

4. Conclusion

A series of Schiff bases, **1a**–**1d**, has been synthesized under mild conditions and characterized by ^{1}H NMR and HRMS spectra. Compounds **1a**–**1c** exhibit a unique proton-transfer tautomer emission, while compound **1d** exhibits remarkable dual emission due to the different solvent-polarity environments between ESICT and ESIPT states. The results make further rational design of the ESICT/ESIPT coupled systems feasible simply by modifying the molecular structures.

Acknowledgment

We thank the National Science Council (No. NSC 101-2113-M-035-001-MY2) for the financial support.

References

[1] S.T. Ha, T.L. Lee, G.Y. Yeap, et al., Mesomorphic behavior of new azomethine liquid crystals having terminal iodo group, Chin. Chem. Lett. 22 (2011) 260–263.
[2] S.H. Kim, I.J. Hwang, S.Y. Gwon, S.M. Burkinshaw, Y.A. Son, An anion sensor based on the displacement of 2,6-dichlorophenol-indo-o-cresol sodium salt from a water-soluble tetrasulfonated calix[4]arene, Dyes Pigm. 88 (2011) 84–87.
[3] L.C. Wu, L.Q. Liu, H.S. Jin, X.L. Zhao, K. Wen, Synthesis and structure determination of pyrazine-containing macrocyclic polyazomethines, Chin. Chem. Lett. 21 (2010) 1263–1266.
[4] V.Z. Shirinian, A.A. Shimkin, D.V. Mailian, et al., 7-Nitro- and 7-aminosubstituted spiropyrans of 1-benzothieno[3,2-b]pyrrole, Dyes Pigm. 84 (2010) 19–24.
[5] F. Deng, W. He, A.S. Luyt, Y.Y. Jiang, Synthesis and properties of a novel polyester containing bithiazole, Chin. Chem. Lett. 22 (2011) 109–113.
[6] T. Aysha, S. Luňák, A. Lyčka, R. Hrdina, Synthesis, absorption and fluorescence of hydrazone colorants based on pyrrolinone esters, Dyes Pigm. 91 (2011) 170–176.
[7] G.K. Karaoğlan, G. Gümrükçü, A. Koca, A. Gül, The synthesis, characterization, electrochemical and spectroelectrochemical properties of a novel, cationic, water-soluble Zn phthalocyanine with extended conjugation, Dyes Pigm. 88 (2011) 247–256.
[8] İ. Değirmencioğlu, E. Atalay, M. Er, et al., Novel phthalocyanines containing substituted salicyclic hydrazone-1,3-thiazole moieties: microwave-assisted synthesis, spectroscopic characterization, X-ray structure and thermal characterization, Dyes Pigm. 84 (2010) 69–78.

[9] V. Arun, S. Mathew, P.P. Robinson, et al., The tautomerism, solvatochromism and non-linear optical properties of fluorescent 3-hydroxyquinoxaline-2-carboxalidine-4-aminoantipyrine, Dyes Pigm. 87 (2010) 149–157.

[10] Y.F. Sun, S.H. Xu, R.T. Wu, et al., The synthesis, structure and photoluminescence of coumarin-based chromophores, Dyes Pigm. 87 (2010) 109–118.

[11] G.K. Karaoğlan, A. Koca, A. Gül, U. Avcıata, Synthesis and characterization of novel soluble phthalocyanines with fused conjugated unsaturated groups, Dyes Pigm. 90 (2011) 11–20.

[12] S.M. Seyedi, R. Sandaroos, G.H. Zohuri, Novel cobalt(II) complexes of amino acids–Schiff bases catalyzed aerobic oxidation of various alcohols to ketones and aldehyde, Chin. Chem. Lett. 21 (2010) 1303–1306.

[13] L. Yin, X. Jia, X.S. Li, Simply air: vanadium-catalyzed oxidative kinetic resolution of methyl o-chloromandelate by ambient air, Chin. Chem. Lett. 21 (2010) 774–777.

[14] Y.L. Yang, N.N. Wan, W.P. Wang, Z.F. Xie, J.D. Wang, Synthesis of bis(indolyl) methanes catalyzed by Schiff base–Cu(II) complex, Chin. Chem. Lett. 22 (2011) 1071–1074.

[15] X.D. Li, M.S. Zhan, Synthesis and mesomorphic properties of bent-shaped molecule with low bent-angle central core and long alkylthio tail, Chin. Chem. Lett. 22 (2011) 1111–1114.

[16] S.T. Ha, L.K. Ong, S.L. Lee, et al., Synthesis and mesomorphic properties of Schiff base esters possessing terminal chloro substituent, Chin. Chem. Lett. 21 (2010) 637–640.

[17] S.T. Ha, K.L. Foo, R.T. Subramaniam, M.M. Ito, S.T. Ong, Heterocyclic benzoxazole-based liquid crystals: synthesis and mesomorphic properties, Chin. Chem. Lett. 22 (2011) 1191–1194.

[18] P.J. Chai, Y.S. Li, C.X. Tan, An efficient and convenient method for preparation of disulfides from thiols using air as oxidant catalyzed by Co-Salophen, Chin. Chem. Lett. 22 (2011) 1403–1406.

[19] A. Benvidi, M.T. Ghanbarzadeh, M. Mazloum-Ardakani, R. Vafazadeh, Iodide-selective polymeric membrane electrode based on copper(II) bis(N-2-bromophenylsalicyldenaminato) complex, Chin. Chem. Lett. 22 (2011) 1087–1090.

[20] S. Malek-Ahmadi, A. Abdolmaleki, Synthesis and characterization of new azo containing Schiff base macrocycle, Chin. Chem. Lett. 22 (2011) 439–442.

[21] S.L. Yu, Y.Y. Li, Z.R. Dong, et al., Synthesis of novel chiral N, P-containing multidentate ligands and their applications in asymmetric transfer hydrogenation, Chin. Chem. Lett. 22 (2011) 1269–1272.

[22] H. Naeimi, K. Rabiei, Mild, convenient and efficient synthesis of novel 2,2-dichloro-1,3-diarylaziridines from Schiff bases by phase transfer CTAB catalysis under low concentration alkaline conditions, Chin. Chem. Lett. 22 (2011) 1273–1276.

[23] Y.L.N. Murthy, N. Karthikeyan, G. Boddeti, B.S. Diwakar, E.R. Singh, Design, synthesis and in vitro antibacterial activities of methyl-4-((substituted phenyl) [6H-indolo(2,3-*b*)quinoxalin-6-yl]methyl-amino)benzoate derivatives, Chin. Chem. Lett. 22 (2011) 567–570.

[24] T.N. Akhaja, J.P. Raval, Design, synthesis, in vitro evaluation of tetrahydropyrimidine–isatin hybrids as potential antibacterial, antifungal and anti-tubercular agents, Chin. Chem. Lett. 23 (2012) 446–449.

[25] X.L. Zhong, F. Gao, Q. Wang, H.R. Li, S.T. Zhang, Excited state intramolecular proton transfer of novel conjugated derivatives containing hydroxy and imino groups, Chin. Chem. Lett. 21 (2010) 1195–1198.

[26] L. Xie, Y. Chen, W. Wu, et al., Fluorescent coumarin derivatives with large stokes shift, dual emission and solid state luminescent properties: an experimental and theoretical study, Dyes Pigm. 92 (2012) 1361–1369.

[27] G.O.W Lins, L.F. Campo, F.S. Rodembusch, V. Stefani, Novel ESIPT fluorescent benzazolyl-4-quinolones: synthesis, spectroscopic characterization and photophysical properties, Dyes Pigm. 84 (2010) 114–120.

[28] C.K. Lim, J. Seo, S. Kim, et al., Concentration and pH-modulated dual fluorescence in self-assembled nanoparticles of phototautomerizable biopolymeric amphiphile, Dyes Pigm. 90 (2011) 284–289.

[29] Y. Ito, K. Amimoto, T. Kawato, Prototropic tautomerism and solid-state photochromism of N-phenyl-2-aminotropones, Dyes Pigm. 89 (2011) 319–323.

[30] Y.J. Zhang, X.P. He, M. Hu, et al., Highly optically selective and electrochemically active chemosensor for copper (II) based on triazole-linked glucosyl anthraquinone, Dyes Pigm. 88 (2011) 391–395.

[31] T. Li, Z. Yang, Y. Li, et al., A novel fluorescein derivative as a colorimetric chemosensor for detecting copper(II) ion, Dyes Pigm. 88 (2011) 103–108.

[32] W.H. Hong, C.C. Lin, T.S. Hsieh, C.C. Chang, Preparation of fluoroionophores based on diamine-salicylaldehyde derivatives, Dyes Pigm. 94 (2012) 371–379.

[33] K.C. Tang, M.J. Chang, T.Y. Lin, et al., Fine tuning the energetics of excited-state intramolecular proton transfer (ESIPT): white light generation in a single ESIPT system, J. Am. Chem. Soc. 133 (2011) 17738–17745.

[34] P.T. Chou, S.C. Pu, Y.M. Cheng, et al., Femtosecond dynamics on excited-state proton/charge-transfer reaction in 4′-N,N-diethylamino-3-hydroxy-flavone, J. Phys. Chem. A 109 (2005) 3777–3787.

[35] M.H. Luo, H.Y. Tsai, H.Y. Lin, S.K. Fang, K.Y. Chen, Extensive spectral tuning of the proton transfer emission from green to red via a rational derivatization of salicylideneaniline, Chin. Chem. Lett. 23 (2012) 1279–1282.

[36] M.J. Chang, T.C. Fang, H.Y. Tsai, M.H. Luo, K.Y. Chen, (*E*)-4-[(4-Diethylamino-2-hydroxybenzylidene)amino]benzonitrile, Acta Cryst. E68 (2012) o904–o905.

[37] G.P. Moloney, R.W. Gable, M.N. Lskander, D.J. Craik, M.F. Mackay, Anomalies in the reduction of the Schiff bases 5-(diethylamino)-2-(phenyliminomethyl)phenol and 2-[(4-diethylaminophenyl)-iminomethyl]-phenol and their crystal structures, Aust. J. Chem. 43 (1990) 99–107.

[38] X.X. Gong, J.H. Xu, 4-(2-Hydroxybenzylideneamino)benzo-nitrile, Acta Cryst. E64 (2008) o1188.

[39] F. Arod, M. Gardon, P. Pattison, G. Chapuis, The α2-polymorph of salicylideneaniline, Acta Cryst. C61 (2005) o317–o320.